Mar Geophys Res (2015) 36:81–98
DOI 10.1007/s11001-014-9231-y

BRIEF REPORT

Quaternary sedimentation and active faulting along the Ecuadorian shelf: preliminary results of the ATACAMES Cruise (2012)

F. Michaud · J. N. Proust · J. Y. Collot · J. F. Lebrun · C. Witt · G. Ratzov · H. Pouderoux · C. Martillo · M. J. Hernández · G. Loayza · L. Penafiel · L. Schenini · A. Dano · M. Gonzalez · D. Barba · L. De Min · G. Ponce · A. Urresta · M. Calderon

Received: 22 March 2014 / Accepted: 9 July 2014 / Published online: 1 August 2014

Abstract Selected high-resolution seismic-reflection profiles and multibeam bathymetry acquired along the convergent Ecuador margin during the ATACAMES cruise on onboard the R/V L'Atalante (Jan.15–Feb.18, 2012) allow a preliminary evaluation of the neotectonic development and stratigraphic evolution of the margin based on the sismo-stratigraphic analysis of Quaternary sediment preserved on the margin shelf and upper slope. We present three major preliminary results. (1) The evolution of the Esmeraldas, Guayaquil and Santa Elena canyons. The head of the Esmeraldas canyon is the location of a continuous significant sediment transport. The Guayaquil canyon shows several episodes of deposition and incision. Aggrading sedimentation pattern in the canyon records several changes in relative sea-level. The subsidence of the Gulf of Guayaquil probably contributes to the good preservation of the canyon filling stages. The Santa Elena canyon is controlled by a SW–NE trending normal fault. (2) Variations of sediment accumulation and relative vertical motions are shown along-strike the shelf edge. Offshore the uplifted Manta peninsula, a pronounced subsidence of the shelf edge is documented by sedimentary clinoforms that have deposited in a morphological reentrant, and have migrated upslope testifying of a local subsidence meanwhile the

F. Michaud · M. J. Hernández
Université Pierre et Marie Curie, Paris, France

F. Michaud (✉) · J. Y. Collot · C. Martillo · M. J. Hernández · L. Schenini · A. Dano · G. Ponce
Geoazur, IRD-CNRS-OCA, Université de Nice-Sophia-Antipolis, 250 Avenue Albert Einstein, 06560 Valbonne/Sophia Antipolis, France
e-mail: micho@geoazur.unice.fr

J. N. Proust · H. Pouderoux · C. Martillo · M. Gonzalez
Géosciences Rennes, CNRS, Université de Rennes 1, Campus de Beaulieu, 35042 Rennes cedex, France

J. Y. Collot
Investigador Prometeo, Instituto Geofísico, Escuela Politécnica Nacional, Ladrón de Guevara E11-253, Ap. 2759, Quito, Ecuador

J. F. Lebrun · L. De Min
Université des Antilles et de la Guyane, Campus de Fouillole, 97159 Pointe à Pitre cedex, Guadeloupe, France

C. Witt
Géosystèmes, Université Lille 1, Avenue Paul Langevin, 59655 Villeneuve d'Ascq cedex, France

G. Ratzov
Domaines Océaniques, Université de Bretagne Occidentale, Place Copernic, 29280 Plouzané, France

C. Martillo · G. Loayza · G. Ponce
Departamento de Geologia, Escuela Politecnica del Litoral, km 30.5 Vía Perimetral Campus "Gustavo Galindo", Guayaquil, Ecuador

M. J. Hernández · L. Penafiel
Departamento de Geologia, Escuela Politecnica Nacional, Ladrón de Guevara E11 – 253, Quito, Ecuador

M. Gonzalez · G. Ponce · M. Calderon
Instituto Oceanografica de la Armada de Ecuador (INOCAR), Avenida 25 de Julio via Puerto Maritimo, Base Naval Sur, Guayaquil, Ecuador

D. Barba · A. Urresta
Petroamazonas, Naciones Unidas E-7-95 y los Shyris, Quito, Ecuador

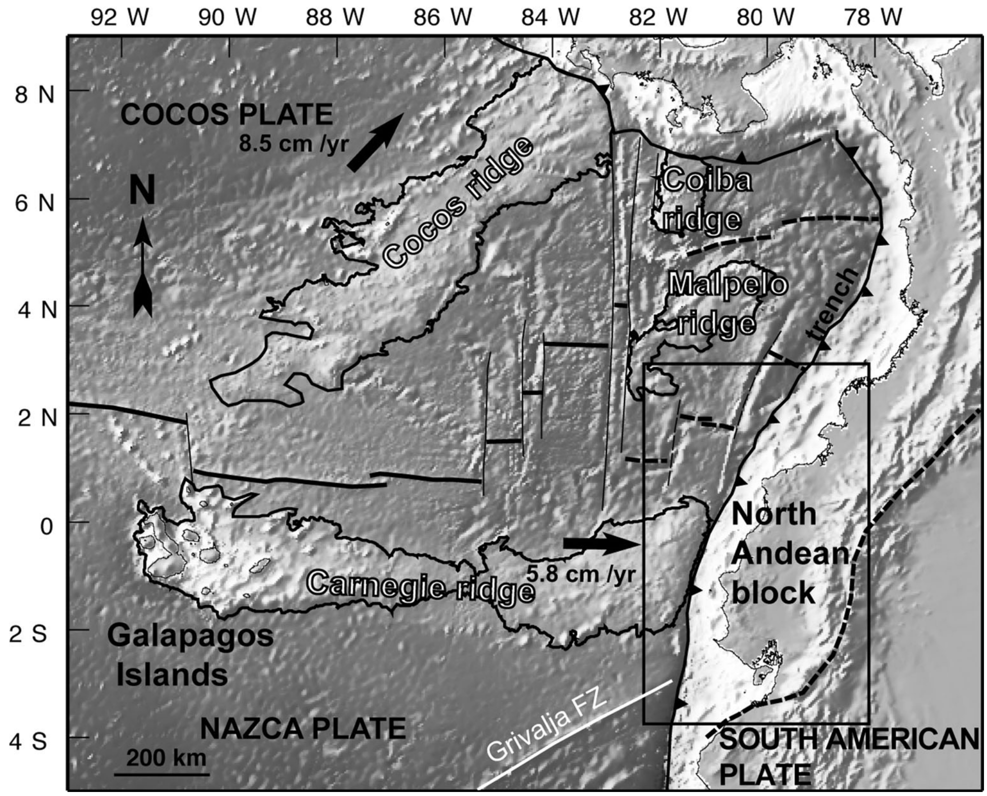

Fig. 1 Geodynamic framework of the study area. The Nazca plate subducts beneath the South American continent at velocity of 5.8 cm/year (Trenkamp et al. 2002). The forearc area is characterized by the arrival in the trench of the Carnegie Ridge and the escape to the North of the North Andean block. Location of the Fig. 2 (*box*). *Dashed line* = eastern boundary of the North Andean block from Bourgois 2013

adjacent La Plata Island area underwent uplift. In the Esmeraldas canyon area, a local uplift of the shelf is documented. (3) Two neotectonic fault systems with a possible transcurrent component are imaged across the shelf edge and upper margin slope offshore Jama, and Cape Galera. This possible transcurrent motion could be related to the reactivation of ancient faults of the upper plate by the subduction. These preliminary results indicate that the ATACAMES data set has a strong potential to evaluate the spatial and temporal contribution of tectonic and climate changes on the structural development and stratigraphic evolution of the Ecuador continental margin.

Keywords Subduction · Sediment supply · Tectonic · Canyon · Fault · Ecuador

Introduction

Active margins represent open systems in which part of the terrestrial sediment flux reaching the trench is bound to be recycled deeper until the Earth's mantle. Although this process loses part of the sedimentary record, a significant fraction of it is nevertheless preserved in the fore-arc and upper slope basins. Investigating this record offers an access to the relative influences of climate and tectonics on the morphogenesis of active margins, particularly during the Pleistocene, when large amplitude variations of sea level have fostered thick sediment preservation on subsiding margins. Accordingly, the ATACAMES cruise was designed to document the fine scale architecture of the Pleistocene sedimentary record and fault systems at the junction between the upper slope and continental shelf of the Ecuador convergent margin.

The Ecuador convergent margin (Fig. 1) is an excellent target to tentatively discriminate the details of the effects of eustatic changes and use the corresponding sedimentary records of climate to study the tectonic evolution. First, subduction erosion and related subsidence of the outer-margin wedge is the geodynamic process that dominates the recent evolution of the 700-km-long margin of Ecuador (Collot et al. 2002; Sage et al. 2006; Collot et al. 2008); this regional subsidence facilitates the sedimentary accumulation and record. Second, in response to the Carnegie Ridge subduction (Collot et al., 2009) the margin recorded a Plio-Pleistocene segmentation of the continental slope (Gutscher et al. 1999; Collot et al. 2009) (Fig. 2). The central segment (between latitude N1° and latitude S2°30′), which is the main target of this study, shows a narrow shelf, a steep margin slope and a trench devoid of sediment (Sage et al. 2006). On both sides are two subsiding segments with ensconced sedimentary basins (Fig. 2): the Gulf of Guayaquil to the south (Witt et al. 2006) and the Manglares basin to the North (Marcaillou and Collot 2008). Since the

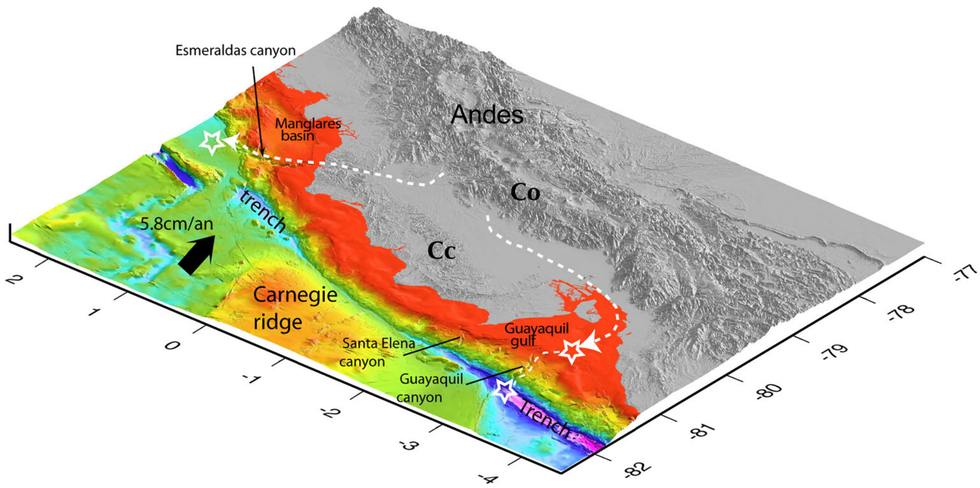

Fig. 2 In Ecuador the uplift of the Andes (Western Cordillera = Co) is the main source of detrital material transported to the trench. The Coastal Cordillera (Cc), whose uplift is most likely related to the entrance of the Carnegie Ridge in the subduction zone, constitutes a barrier for the Andean drainage for nearly 700 km along the margin. The drainage from the Andes is now diverted (a) to the Rio Esmeraldas in the North that transfers sediment coming into the trench through the Esmeraldas canyon; and (b) to the Rio Guayas in the south that transfers sediment arriving in the Gulf of Guayaquil to the trench through the canyon of Guayaquil. Current sediment transport pathways are represented by *white dashed lines*; *white stars* = principal actual site of sediment accumulation along the margin. Convergence velocity of the Nazca plate/South America according to Trenkamp et al. 2002. Bathymetry from Michaud et al. 2006

Plio-Pleistocene, uplift of the coastal cordillera has shut down the sediment supply from the Andes to the central margin segment (Fig. 2). Consequently the two subsiding segments drain most of the sediment flux from the Andes through the Guayaquil and Esmeraldas submarine canyons (Collot et al. 2009).

The ATACAMES geophysical cruise conducted onboard the research vessel L'Atalante (Ifremer) in January–February 2012 acquired high-resolution multichannel seismic-reflection and 3.5 kHz mud penetrator (Chirp) data in 100–1,000 m water depths, together with multibeam bathymetry and piston cores along the entire Ecuador margin (Fig. 3). In this paper, we chose to present only selected HR seismic reflection lines and bathymetric data that support three major discoveries of the ATACAMES cruise: (1) The recent history of the incision and infilling of the Esmeraldas, Santa Elena and Guayaquil submarine canyons at the shelf edge, (2) the along-strike variation of the relationship between recent sea level fluctuations and margin vertical tectonics, and (3) some remarkable likely active faults that cut across the shelf.

Geodynamic context

The Nazca plate underthrusts eastward the Ecuadorian margin, at 5.6–5.8 cm/year relative to the South American plate (Trenkamp et al. 2002; Nocquet et al. 2009). The basement of the coastal area of Ecuador consists of accreted oceanic terranes (Jaillard et al. 1997). The subduction of the Carnegie Ridge (Gutscher et al. 1999; Michaud et al. 2009; Collot et al. 2009) and the northward escape of the North Andean block relative to the South American Plate (Witt et al. 2006; Trenkamp et al. 2002; Nocquet et al. 2009) (Fig. 1) control the geologic evolution of the margin. Across the forearc, the uplift of the coastal cordillera diverts the sediment supply from the Andes to the north and to the south (Collot et al. 2009). The drainage from the Andes is now diverted (a) towards the Rio Esmeraldas in the North that transfers sediment into the trench through the Esmeraldas canyon; and (b) towards the Rio Guayas in the south that transfers sediment in the Gulf of Guayaquil and to the trench through the canyon of Guayaquil (Fig. 2). The coastal uplift (Pedoja et al. 2006a, b), and part of the coastal range uplift (Gutscher et al. 1999) is inferred to be related to the subduction of the Carnegie Ridge for at least the last 1.3 Ma (Graindorge et al. 2004). Based on a kinematic reconstruction and a morphologic analysis of the margin outer-wedge, Collot et al. (2009) suggested that the Carnegie Ridge subduction initiated 4–5 Ma ago and was fully established by $\sim$2 Ma. The subduction of the Carnegie Ridge or the collision of along-strike positive relief (Witt et al. 2006) is synchronous with he acceleration of the subsidence in the Gulf of Guayaquil (Deniaud et al. 1999) 1.6–1.8 Ma ago, which in turn has been attributed to an increase of the North Andean block escape velocity (Witt et al. 2006). Finally the climate changes during the Pleistocene time appear as the major drivers of the transfers of sediment.

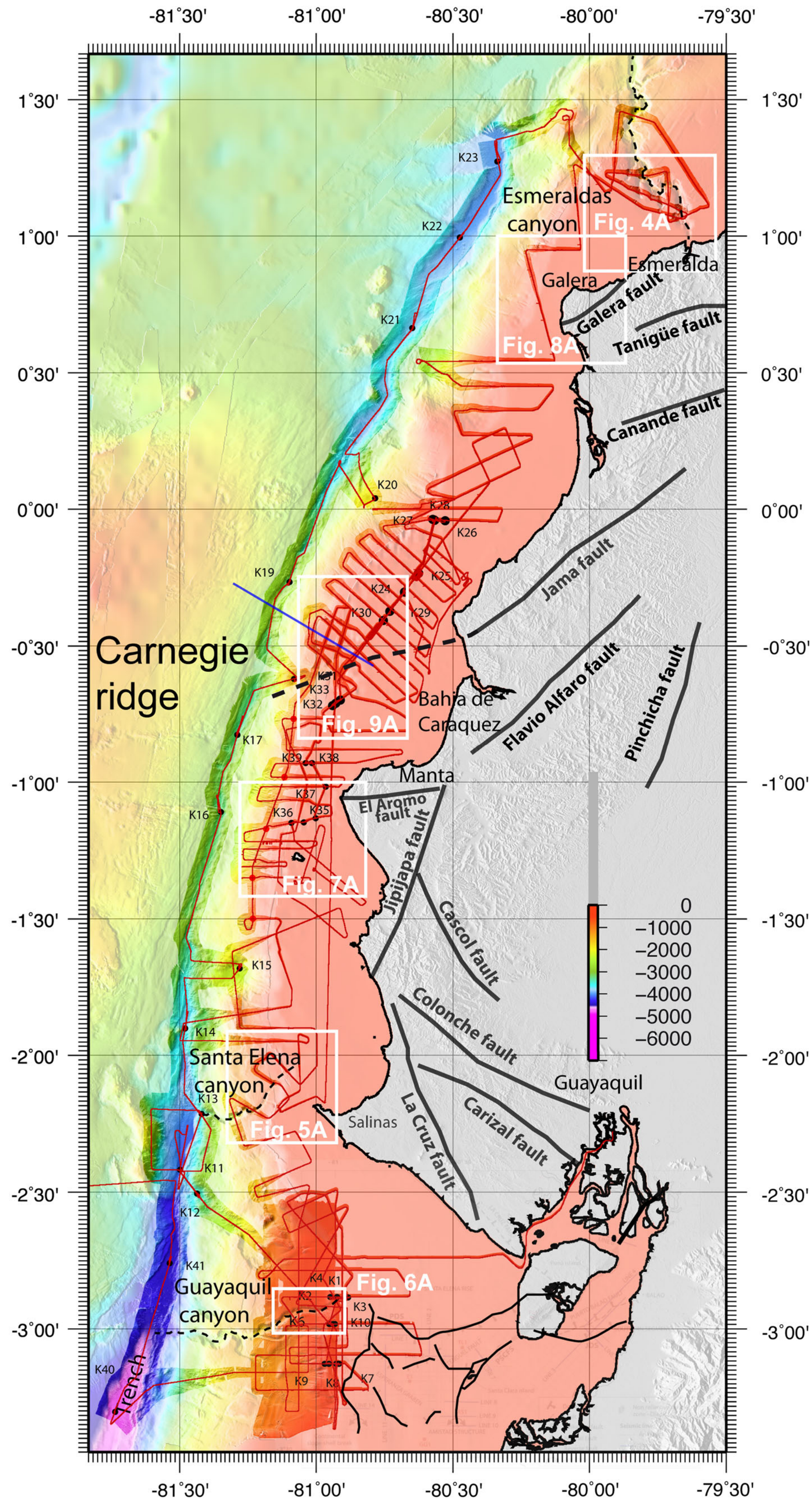

Fig. 3 Details of ATACAMES shiptracks performed on the continental shelf and in the trench (*black circles* marked K = location of cores). The sustained color along the shiptracks = multibeam bathymetry collected during the ATACAMES cruise and/or high resolution seismic and chirp data. *Red lines* = ATACAMES shiptracks. *Black lines* = principal faults on land from Reyes and Michaud, 2012; Offshore faults in the Gulf of Guayaquil are from Witt et al. 2006. *Thick doted black line* = prolongation offshore of the Jama fault inferred by Collot et al. 2004 based on one seismic profil (*blue line*). Thin doted black lines = canyon axes

Methods

High-resolution multibeam bathymetric data were obtained during the ATACAMES cruise using a Kongsberg EM122 and EM710 Simrad multibeam echosounder, allowing a digital elevation model with a grid spacing of 25 m to be constructed using the seafloor mapping software CARAIBES (TM Ifremer). Seismic reflection data were recorded using a 72-channels digital streamer towed at 2 m of water depth (channel length 6.25 m). The source array towed at 2.1 m of water depth consisted of two ramps mounted with three 13/13 Ci plus three 24/24 Ci mini GIgun. Shots was fired at 140 bars every 25 m. Given this shot rate and the streamer configuration this seismic reflection system ensure a nine fold stack. The seismic lines were processed on board with the Seismic Unix (SU) software (Center of Wave Phenomena, Colorado School of Mines) for Band Pass Filtering, spherical divergence correction (water velocity)—NMO velocity analysis and correction, nine fold stack and constant velocity time migration (1,490 m/s).

The seismic profiles were interpreted applying the criteria of the seismic stratigraphy (Mitchum et al. 1977): configuration, amplitude, continuity and frequency for identifying the seismic facies, and the stratal terminations (Vail et al. 1977) for definition of seismic unit (U). Seismic unit numbering (Ux) is specific to each profile.

The canyons of the Ecuadorian margin

The three main submarine canyons of the Ecuadorian margin, are the Esmeraldas, Santa Elena and Guayaquil canyons (Fig. 3). The two main rivers Guayas and Esmeraldas rivers draining the Andes and bypassing the coastal Cordillera down cut the Guayaquil and Esmeraldas canyons respectively to the south and to the north of the Ecuador margin (Fig. 2). The Esmeraldas canyon cuts the shelf up to the coast (Collot et al. 2005) whereas the Guayaquil canyon cuts the continental shelf edge of the Gulf of Guayaquil far away (50 km) from the coast. The Santa Elena canyon (Fig. 3) is located 35 km west of the coastline. It faces the southern wedge of the coastal Cordillera but it is not presently associated with any significant river (Fig. 2) or a large onland watershed. The collection of an homogeneous new set of seismic and multibeam data on the shelf and the upper slope cutting across these three canyons obtained during the ATACAMES cruise foster the comparison of their sedimentary architecture and relation to sea level variations and tectonics.

Esmeraldas canyon

The Esmeraldas canyon is $\sim$130 km-long. The canyon is installed at the boundary between the Manglares fore-arc basin (Marcaillou and Collot, 2008) and a wide, less than 50-m-deep, shelf promontory (Collot et al. 2004) (Fig. 4A). Previous multibeam bathymetric data show that the canyon sharply cuts the deformation front of the incipient accretionary wedge in the trench at a $\sim$2,750 m of water depth, thus indicating high current transport activity (Collot et al. 2005, 2008). From the mouth of the Esmeraldas River until the upper slope the canyon shows both linear and highly sinuous segments with a remarkable and abrupt change in direction from NS to NW–SE. Previous seismic profiles shot on the middle to lower slope revealed that segments of the canyon are tectonically controlled (Collot et al. 2006a, b; Silva et al. 2006; Silva 2007).

New data from ATACAMES cruise on the upper slope and the shelf show that the shelf break is located at 140 m in water depth west of the shallow shelf promontory (Fig. 4a). Eastward, near the Esmeraldas canyon, the shelf break is located at 110 m in water depth. Three NS-trending tributaries incise the upper slope and breach the shelf break. From west to east, the incision of these tributaries increases in depth, the Esmeraldas canyon showing the greatest incision, and their heads progressively shifts eastward and landward (Fig. 4a). Indeed, along the upper slope, the steep 300 to 800-m-high walls of the Esmeraldas canyon indicate a powerful erosive activity.

The new NS-trending, profile ATAC-P028 (Fig. 4b) perpendicular to the continental margin and upper slope shows two main geologic domains separated by the Esmeraldas canyon. The northern part corresponds to the Manglares basin (Fig. 4a), whereas the southern part corresponds to the continental shelf. In the northern part, we identify two seismic units (U1 and U2) and five in the southern part (U1 and U3 to U6). U3 to U5 are affected by numerous subvertical normal faults. U3 to U5 boundaries are slight angular, subparallel unconformities deeping in a seaward direction. The U3-U5 units are deeply incised by an irregular surface at the base of U6, which underlines a paleocanyon floor (0-300 CDP, Fig. 4b). U3-U4 show deformed reflections when U5 exhibits well-stratified oblique reflections prograding in a seaward direction (Fig. 4b), which are onlapped by U6 basal reflections.

Santa Elena canyon

The $\sim$40 km-long Santa Elena canyon, is located west of the Santa Elena peninsula (Fig. 5a). The canyon cuts obliquely the upper slope with a SW–NE trend. At water depths over 800 m, the canyon walls are steep with elevations reaching 700 m and the contact between the toe of the slope and the trench is very sharp and not sealed by sediments (Collot et al. 2006b) (Fig. 3). These previous observations suggest that the current activity is strong on

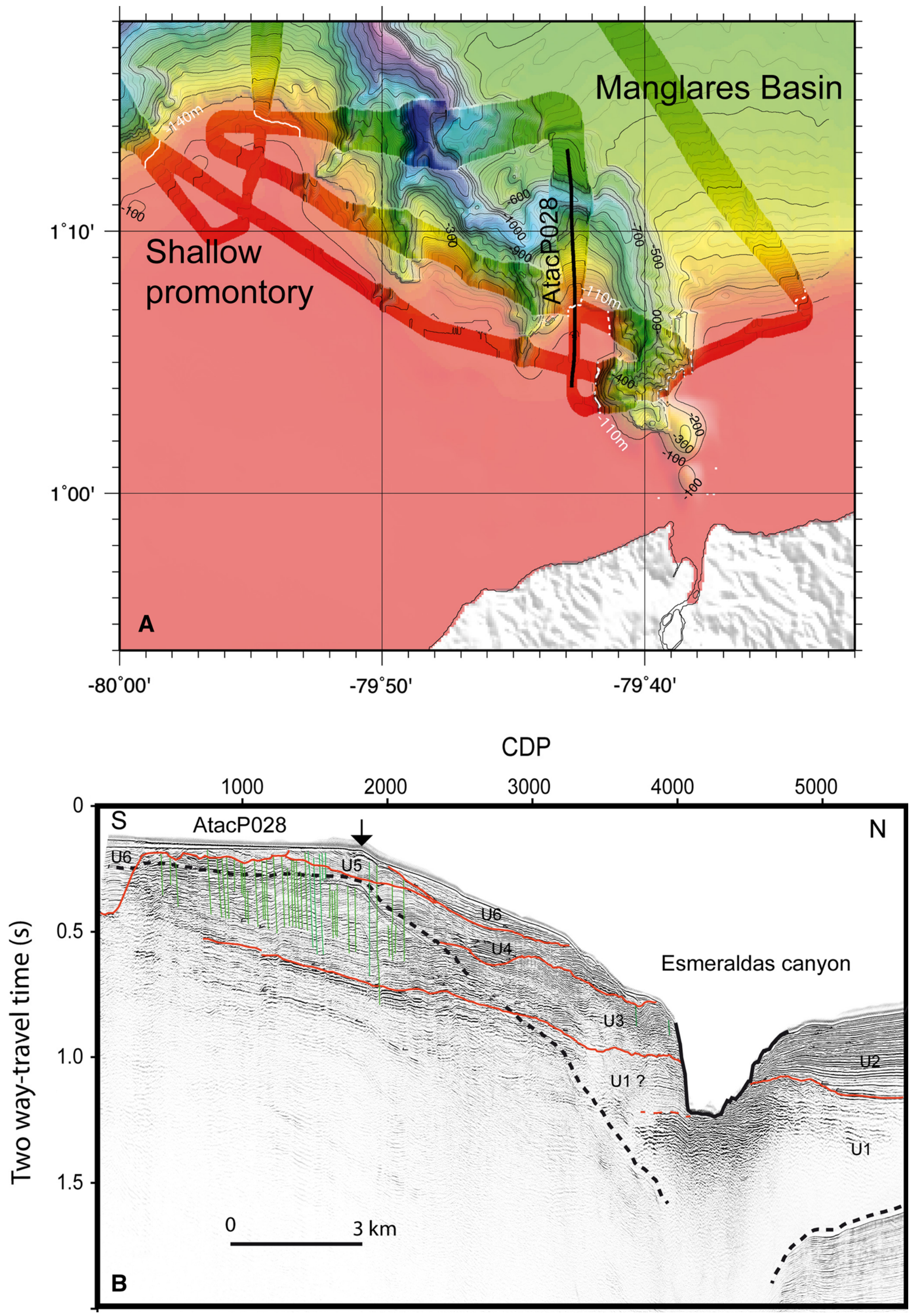

Fig. 4 **a** Bathymetric map of the head of the Esmeraldas submarine canyon (location on Fig. 3). More intense color corresponds to multibeam data acquired during the campaign ATACAMES with contours every 10 m. Less intense color with curves every 20 m = older multibeam data from Michaud et al. 2006; less intense color with curves every 100 m = area with no multibeam bathymetric data. Around the shallow promontory the white contour line corresponds to the isobath −140 m contoured from ATACAMES data, which is located at the break in slope between the platform and the slope (= shelf break). The white dotted line corresponds to the isobaths −110 m contoured from ATACAMES data around the Esmeraldas canyon (−79°40′), where this line is located at the shelf break. *Thick black line* = location of the seismic profile described in this paper; *thin red lines* = ship track during the ATACAMES cruise. **b** Seismic profile shot perpendicular to the Esmeralda canyon (location Fig. 4a). *Red lines* are limits between units; *black line* is the incision of the canyon. *Thick black dashed line* = sea-bottom first multiple. *Black arrow* = shelf break

the slope where the canyon walls are elevated and the thalweg devoided of sediment.

New multibeam data from ATACAMES show that the canyon trend turns to the NNE along its upper course (Fig. 5a). Upslope the canyon terminates on a smooth seafloor looking like a shallow amphitheater, the shelf break sited at 140 m in water depth. The canyon walls are smooth and the thalweg is flat which indicates that the activity is probably low at the canyon head.

New seismic line ATAC-P110 (Fig. 5b) cuts across the Santa-Elena NNE canyon upper course and shows two domains. On the southeastern part of the line (from CDP 5,700 to 3,700), a slightly folded stratified unit (Ub) presents clear seaward dipping reflectors truncated upslope by the seafloor reflector. This thick and deformed unit Ub might correspond to the Paleocene sedimentary basement that outcrops along the nearby coast (Reyes and Michaud 2012). Unit Ub is affected by F1 and F2 major seaward dipping normal faults. F2 offsets the sea floor (Fig. 5b). The northwestern part of the seismic line (from CDP 0 to 2,500) exhibits two well-stratified sedimentary units that overlay a deeper unit which facies resembles that of Ub but dipping in a landward direction. The lower unit (U1) shows deformed and faulted fan-shape strata dipping landward likely limited by the large fault F1. A poorly deformed unit U2 dips seaward and drapes unit U1 indicating that most probably fault F1 is less active since the deposition of unit U2. Between the two domains, the Santa Elena canyon shows three phases of canyon cut-and-fill (i1 to i3, Fig. 5b) below the present day canyon incision. At the time of U1 deposition, the canyon location was mainly driven by the activity of fault F1: the oldest cut-and-fill structure (i1, Fig. 5b) formed before the deposition of the draping unit U2. The chaotic sediment infilling of incision 2 (i2, Fig. 5b) suggests that the fault was still active at that time. Moreover the incision 3 affects the base of unit U2 indicating a last stage of activity of the canyon. The present day canyon floor shows a small flanking levee (Fig. 5b) on the edge of a very narrow flat bottom channel suggesting a low activity of the canyon (Fig. 5b). This suggests that sediment transfer in the canyon is probably very low today.

Guayaquil canyon

The Gulf of Guayaquil is characterized by a 50 km wide continental shelf incised by the ~70 km-long Guayaquil canyon is (Fig. 3) which was mapped all along the slope down to the trench (Collot et al. 2006b).

The ATACAMES multibeam bathymetric data, which add on to EM 302 bathymetric data of the R/V Orion of the INOCAR (Oceanographic Institute of Ecuador), show that the canyon head forms a large amphiteatre disconnected from the present day shoreline (Fig. 6A). The shelf break is located at 160 m of water depth. From the shelf break at 160 m until 800 m in water depth, the canyon trends E–W. Along this segment, from 500 m in water depth onwards the walls of the canyon are 200 m-high. Then the canyon hooks NE–SW further downslope (Fig. 6a). Along the E–W canyon segment, the narrow and sharp thalweg lies at the foot of the canyon northern flank, whereas a terrace lies against its southern flank. Along the NE–SW segment, the thalweg is less prononced. The edges of the canyon are affected by slope scarps and reentrants which constitute possible sources of mass wastings.

The NS trending seismic profile ATAC-P119 cuts across the upper course of the Guayaquil canyon (Fig. 6b). The profile shows that the margin slope is comprised of by six seismic-stratigraphic units (U1 to U6) deeply incised by the canyon. The units thin out southward of the canyon where U1 appears folded. The units exhibit three main seismic facies from bottom to the top: (1) a low amplitude to quasi-transparent facies, (2) a high amplitude chaotic facies, and (3) a medium amplitude well layered facies. The three facies are interpreted respectively as the signature of (1) mass flow deposits, (2) high-density turbidite and channel deposits and (3) low-density turbidite to hemipelagite sediments. The sediment fill of the canyon shows compound fill corresponding to multiple, superimposed cycles of incision and deposition. The canyon displays five main erosion phases and five sediment-fills episodes (f1–f5 Fig. 6b). The sediment-fill units are deposited on the northern and southern sides of the canyon and, exhibit a rise in the base level of incision (Fig. 6b) indicative of an overall aggradational to retrogradational sediment deposition trend. The low angle to subhorizontal reflectors of the last canyon filling episode exhibits high amplitude reflectors at the base, which probably correspond to coarse and heterolithic material. The top of this infilling showing low amplitude reflectors probably corresponds to fine-grained homogeneous sediment. The inferred nature of this last-filling unit shows that sediment transfer in the canyon is probably very low today.

Upper slope and continental shelf sedimentation: the Manta-La Plata area

Shelf break geometry of the Manta-La Plata area

This area includes the shelf in front of the Manta peninsula and La Plata Island. (Fig. 7a). Landward of this area, eight marine terraces at elevations of 25–360 m cover the main part of the Manta peninsula (Pedoja et al. 2006b). Southwest the La Plata Island area has been uplifted, where four marine terraces at elevations ranging from 47 to 160 m are present; on the Plata Island, the marine terraces were cut in the basalts and dolerites of the Pinon Formation (Cantalamessa and Di Celma 2004; Pedoja et al. 2006a).

Despite a partial coverage, the new ATACAMES multibeam data, the location of the shelf break clearly shows two morphologically different areas (Fig. 7a). From latitude S1°22′ to S1°10′, west of La Plata Island, the shelf break is well defined at 140 m in water depth (Fig. 7a). At theses latitudes, the shelf is 40–50-km wide. In contrast, north of latitude S1°10′ and until S1°00′, west of Manta peninsula, the part of the shelf shallower than 140 m is just 5 km-wide. There, the upper slope exhibits a 35 km-large re-entrant (Fig. 7a) and a slope break which occurs at 500 m water depth.

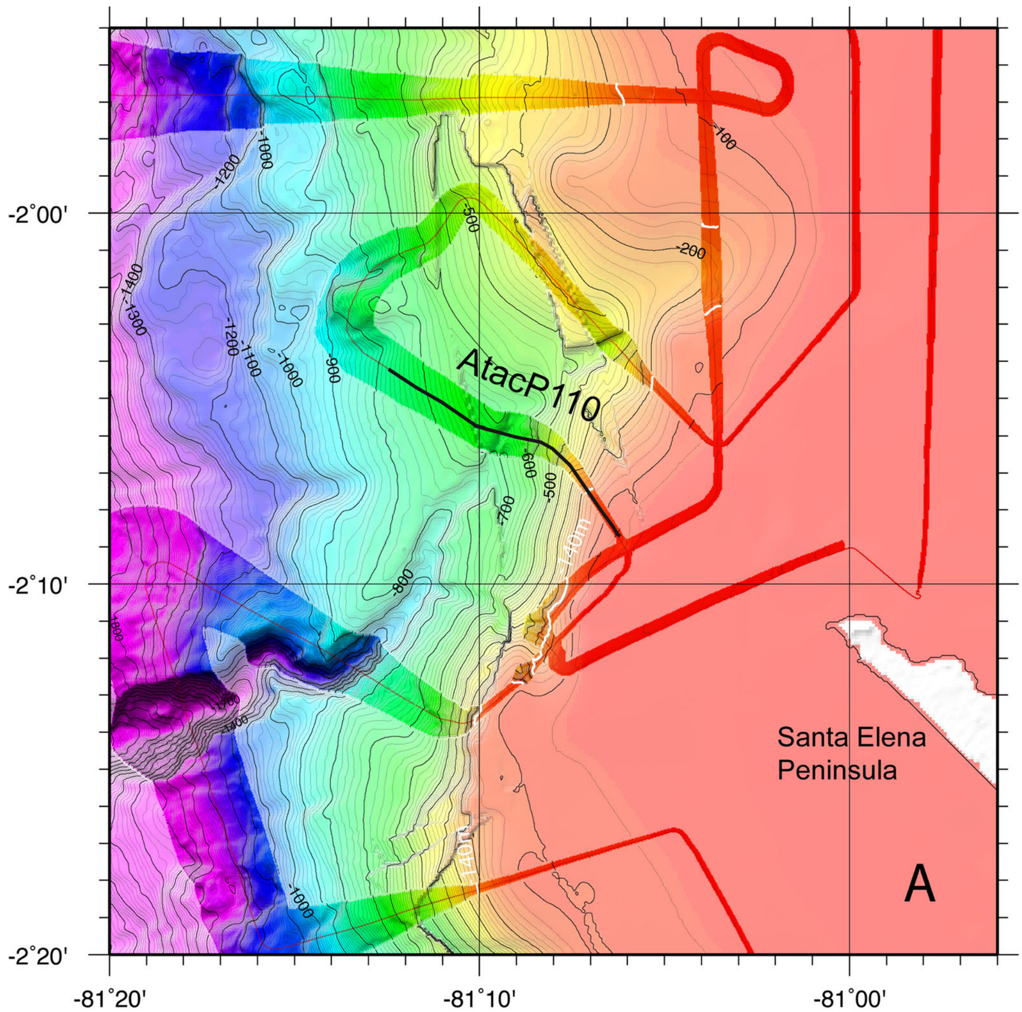
-2°00'
-2°10'
-2°20'
-81°20'
-81°10'
-81°00'
AtacP110
Santa Elena
Peninsula
140m
A

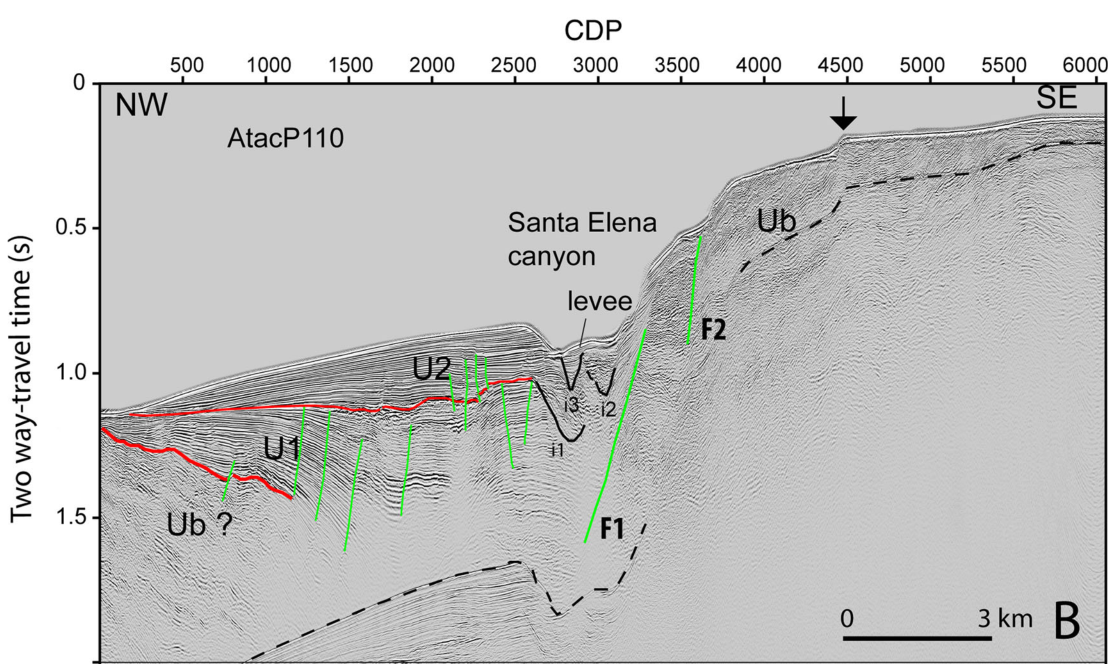
CDP
500 1000 1500 2000 2500 3000 3500 4000 4500 5000 5500 6000
Two way-travel time (s)
0
0.5
1.0
1.5
NW
SE
AtacP110
Santa Elena
canyon
levee
Ub
U2
U1
Ub ?
F1
F2
i1
i2
i3
0
3 km
B

◀**Fig. 5** **a** Bathymetric map of the head of the Santa Elena submarine canyon (location on Fig. 3). More intense color corresponds to multibeam data acquired during the campaign ATACAMES with contours every 10 meters. Less intense color with curves every 20 m = older data from Michaud et al. 2006. The white contour line corresponds to the isobath −140 m contouring from ATACAMES data (shelf break). *Thick black line* = location of the seismic profile described in this paper; thin red lines = ship track during the ATACAMES cruise. **b** Seismic profile across the Santa Elena canyon (location Fig. 5a). *Red lines* are limits between units; *black lines* are the successive incisions of the canyon. *Thick black dashed line* = sea-bottom first multiple. *Black arrow* = shelf break

Manta peninsula subsiding area

In front of Manta peninsula, the E–W-oriented profile ATAC-P092 (Fig. 7b) was shot across the upper slope and continental shelf. A basal unit (Ub) consists of reflection free to low amplitude reflectors with a chaotic configuration. This unit images the acoustic basement of the margin. The Ub Unit is overlain by several well-stratified units (U1 to U13), which consist of medium to high amplitude and continuous reflectors. Some of these units (U5 to U10) exhibit similar geometries including oblique tangential and prograding reflectors, truncated at the top by low angle sub horizontal reflectors. U5 to U10 are growing younger, and stepping landward.

La Plata Island uplifted area

The EW-trending profile ATAC-P098 that extends immediately south of La Plata Island (Fig. 7c) shows a highly deformed unit Ub with chaotic reflectors. This basal unit is seismically equivalent to the basal unit described along the profile ATAC-P092. At CDP 4,300 (Fig. 7c), near the shelf break, a unit of well-stratified oblique reflections dips trenchward suggesting a progradational depositional pattern.

Evidence for neotectonic faults

Evidences for faults activity on the shelf and upper slope are presented below from the area of Punta Galera to the Gulf of Guayaquil area (Fig. 3).

Punta Galera faults

Offshore cape Galera in Northern Ecuador, the few multibeam bathymetric lines show that the shelf break is well marked at 140 m in water depth (Fig. 8a). At latitude N0°50′, the upper margin slope (500 mbsl) is affected by a 40-m-high scarp trending SW-NE and facing Southeast, toward the coast (Fig. 8a, b).

The seismic profile AtacP034 (Fig. 8b) crosses the upper slope from a water depth of ~750 m up to the shelf. Beneath the shelf edge the acoustic basement Ub is dominantly transparent. From the shelf break to the upper slope, Units U1 and U5, which are interpreted as prograding sedimentary clinoforms, are cut vertically by fault F1. Deposits of Unit 4 progressively bury the F1 fault scarp. The folded geometry of the reflectors at the top of U1 next to the fault indicates some contraction meanwhile the seaward dipping geometry of the fault and the vertical offset of the top of Ub indicate a major normal component. At CDP 28,000 (Fig. 8b) and latitude 0°50′ (Fig. 8a), the upper slope of the margin at 500 mbsl, is affected by a SW–NE trending landward dipping fault expressed at the sea bottom by a 40-m-high scarp facing toward the coast. The vertical offset of U1 indicates a normal component along this fault. Normal faults F1 and F2 bound a slope basin filled by Unit 2 and 3. Taken collectively, faults F1 and F2 bound a graben like structure, which controls the subsidence of the upper slope.

Jama fault

Offshore the onland Jama fault (Fig. 3), Collot et al. (2004) interpreted a flower structure as a major crustal transtensional strike-slip fault, trending NE-ward to the offshore west of Bahia de Caraquez (Fig. 3).

The ATACAMES multibeam data, between latitudes S 0°40′ and S 0°20′, exhibit a morphologic re-entrant of the shelf (Fig. 9a) that delimits a 500–600-m-deep ledge. This ledge contains to the North, a 100 m-high rough relief oriented EW (RR on Fig 9a) and, to the South, an arcuate depression.

Seismic profile Atac-P057 crosses the northern boundary of the ledge (Fig. 9b). Between CDP 14,000 and CDP 8,000, the shelf section exhibits a major erosive unconformity that separates a compressively deformed unit (U1) from an overlying undisturbed and well-stratified unit (U2). Near the inboard edge of the ledge described above, U2 is affected by steeply dipping faults, some of which affect the seabed. These faults limit a sedimentary basin that is ensconced in the re-entrant and contains up to 0.5 s twtt of well-stratified sediment (U3). Unit 3 sedimentary infill comprises several sub-units that could be contemporaneous to unit 2 identified on the shelf. The seaward boundary of this basin is characterized by a unit with chaotic seismic facies (U4), which corresponds to the rough EW elongated reliefs on the sea-bottom (RR on Fig. 9a); we interpret this facies as strongly deformed rocks bordering the basin to the west. The dip geometry of the faults that bound the basin indicates that they may merge downward.

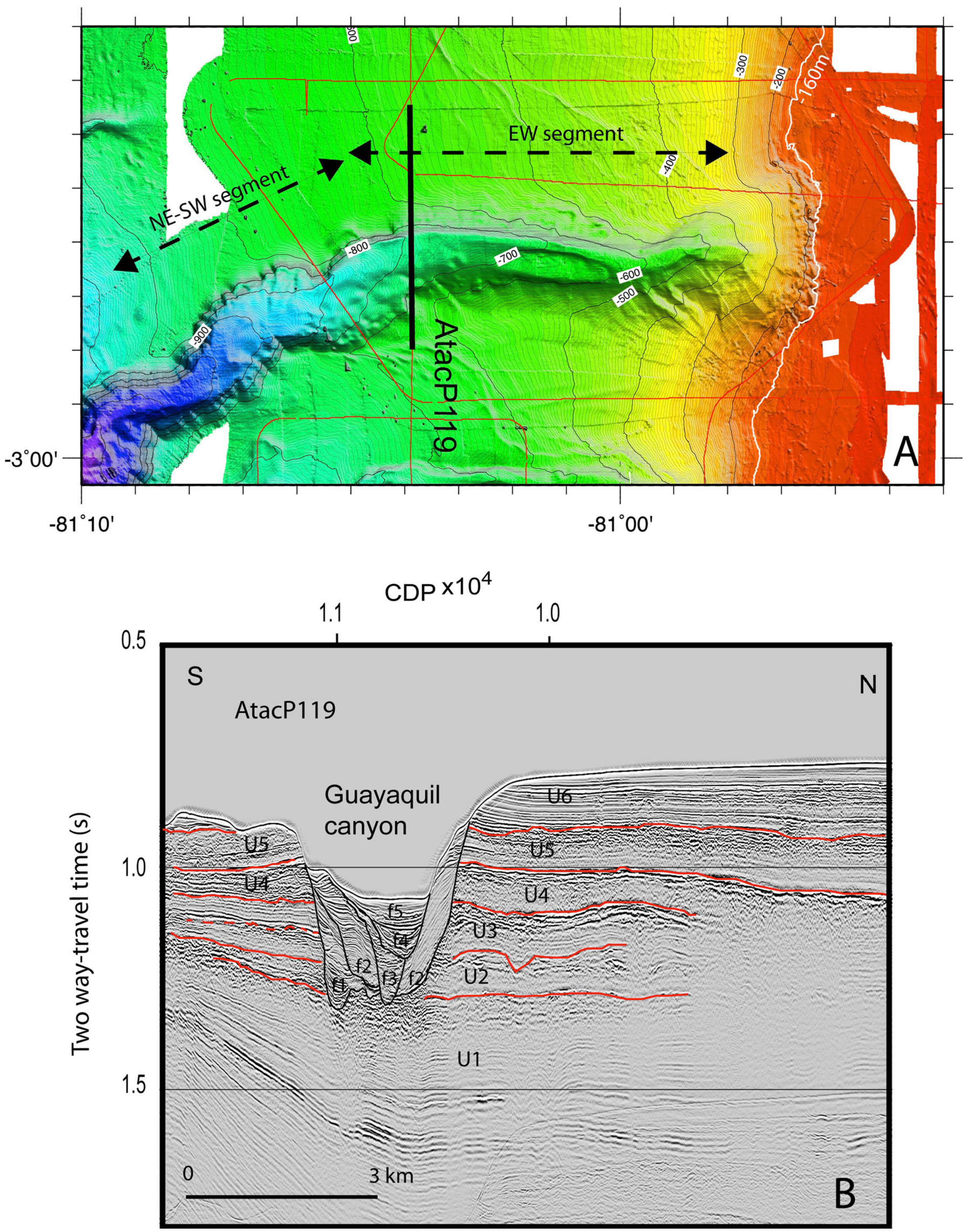

Fig. 6 **a** Bathymetric map of the upper course of the Guayaquil submarine canyon (location on Fig. 3) combining data obtained during the campaign ATACAMES and various INOCAR (Instituto Nacional de Oceanografia de la Armada) cruises, with contours every 5 m. The *white contour line* corresponds to the isobath −160 m contoured from ATACAMES data, which is located at the break in slope between the platform and the slope (= shelf break). *Thick black line* = location of the seismic profile described in this paper; thin *red lines* = ship track during the ATACAMES cruise. *T* = terrace supposed. **b** Seismic profile across the Guayaquil canyon (location Fig. 6a). *Red lines* are limits between units; *black lines* are the successive incisions of the canyon. f1 to f5 = sedimentary filling stages

Discussion

Canyons

Glacioeustatic sea-level control is particularly efficient on the sediment transport through canyons along passive margins with no or little vertical seafloor motion (Posamentier et al. 1991) as well as on active margins with large tectonic deformation rates (Proust and Chanier 2004; Paquet et al. 2011, 2009). Although sea-level acts on both passive and active margins, tectonic deformation could exert a control on Ecuadorian canyon evolution (Ratzov, et al. 2012). Our data confirm that the upper course of the Esmeraldas canyon is devoid of sediments suggesting that significant sediment bypass to the trench. In the Esmeraldas area, the shelf is very narrow and the uplift is significant (Pedoja et al. 2006b). As a consequence, the sediment input can be sustained during periods of relative highstand on a steeply deeping canyon floor flushing sediments to the trench. On the contrary the Guayaquil canyon shows a succession of episodes of deposition and incision. The shelf is very wide over 80 km large. Most of the detrital material was trapped on the shelf during high stands of sea level as today and, on the contrary, bypassed the shelf feeding directly the trench through the Guayaquil canyon during low stands of sea level. The aggrading canyon floor records a relative rise of base level showing that the bulk of the infill might correspond to sediments preserved during late lowstand to early transgressive times. Moreover the subsidence of the Gulf of Guayaquil (Witt et al. 2006)

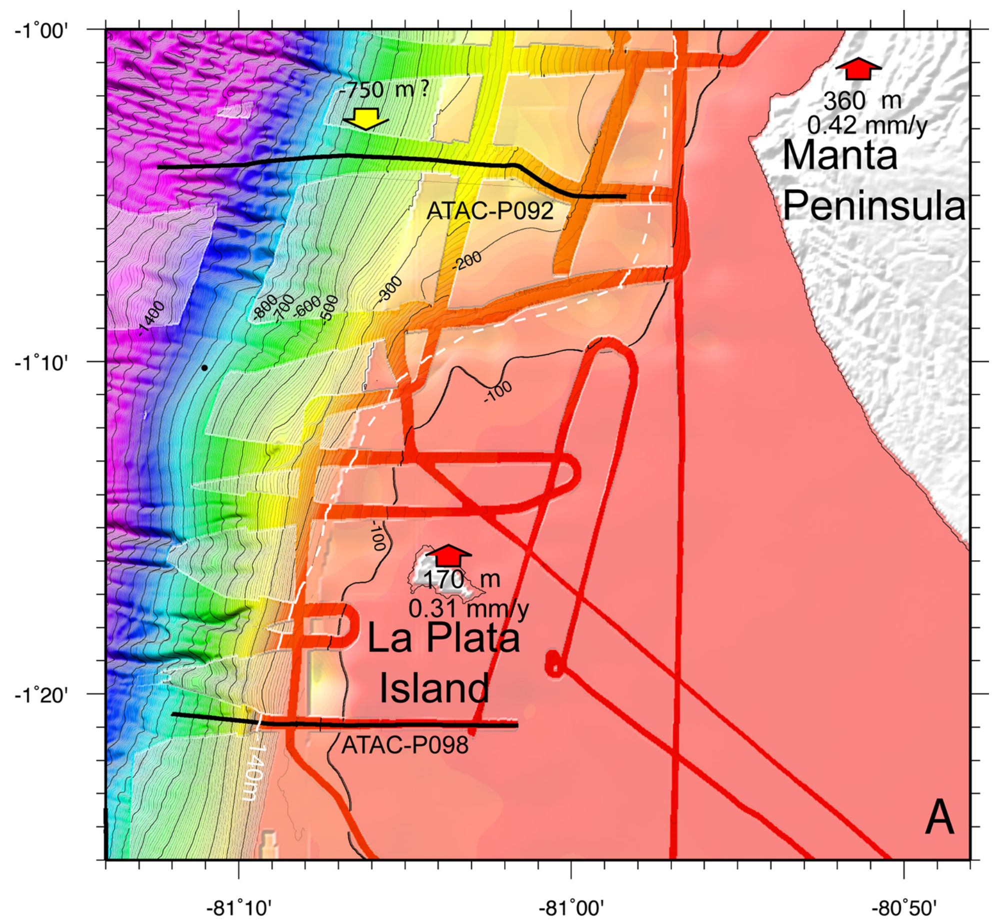

Fig. 7 **a** Bathymetric map of the continental platform of the La Plata Island- Manta peninsula area (location on Fig. 3). More intense color corresponds to multibeam data acquired during the campaign ATACAMES with curves every 10 m. Less intense color with curves every 10 m = older multibeam data from Michaud et al. 2006; less intense color with curves every 100 m = area without multibeam. The *white contour line* corresponds to the isobaths -140 m contoured from ATACAMES data. This depth corresponds to the shelf break in front of La Plata Island; this depth draw a large re-entrant in front of Manta peninsula. The uplift rates on land are from Pedoja et al. (2006b). *Thick black lines* = location of the seismic profiles described in this paper; fine red lines = ship track during the ATACAMES cruise **b** Seismic profile (uninterpreted and interpreted versions) front of the Manta peninsula (location Fig. 7a). *Thick black dashed line* = sea-bottom first multiple. **c** Seismic profile front of the La Plata Island (location Fig. 7A). *Red lines* are limits between units; green lines are faults. *Thick black dashed line* = sea-bottom first multiple. *Black arrow* = shelf break

Fig. 7 continued

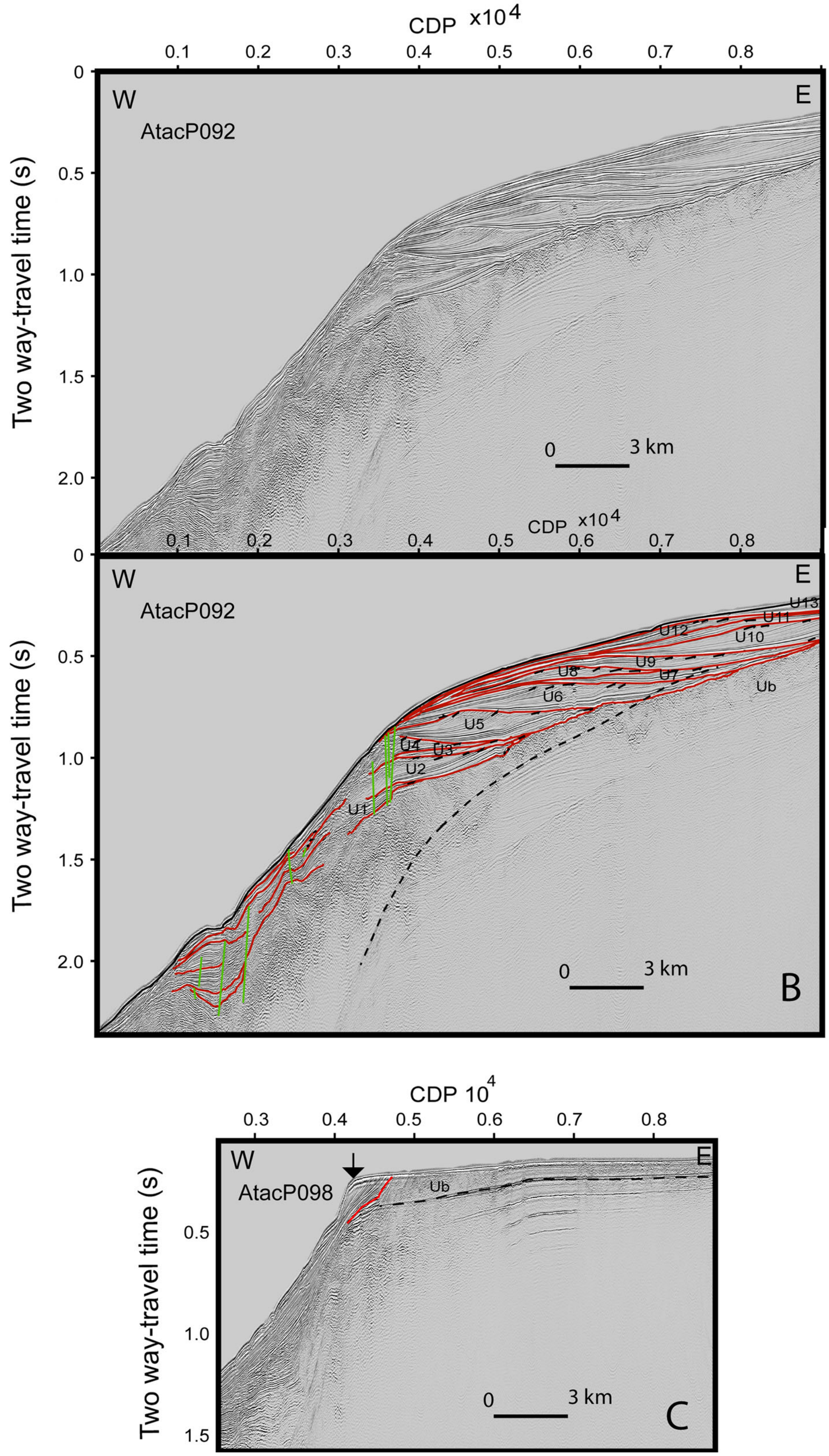

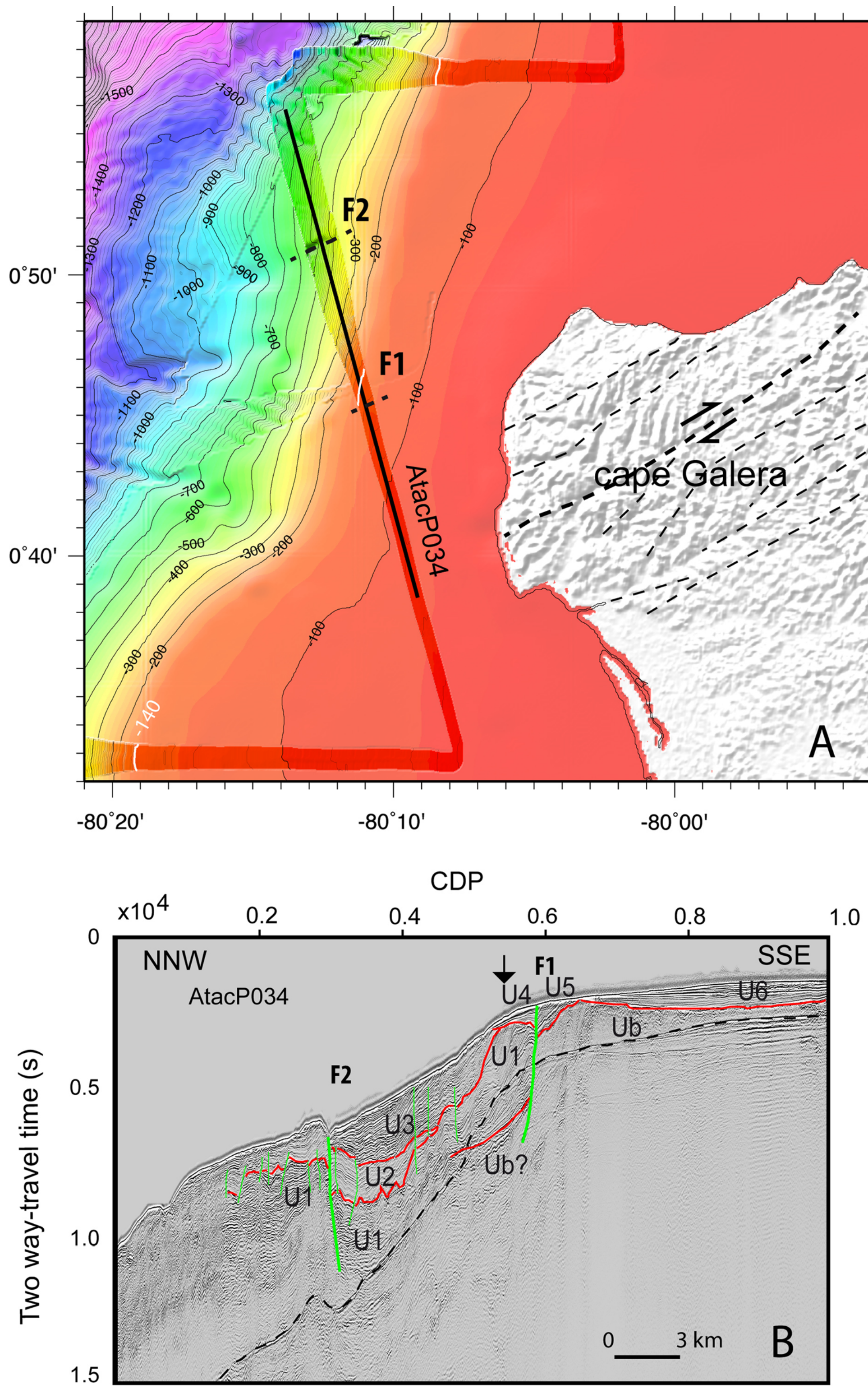

Fig. 8 **a** Bathymetric map of the continental platform in front of the Cape Galera (location on Fig. 3). More intense color corresponds to multibeam data recorded during the campaign ATACAMES with curves every 10 m. Less intense color with curves every 20 m = older multibeam data from Michaud et al. 2006; less intense *color* with curves every 100 m = area without multibeam. The white contour line corresponds to the isobaths −140 m contoured from ATACAMES data (= shelf break). F1 and F2 correspond to the location of faults shown on the seismic lines. Onshore the dashed lines correspond to faults from Reyes and Michaud 2012; the *thickest dashed line* and the strike slip motion (= Galera fault) are from Eguez et al. 2003. Offshore the light dashed lines correspond to the faults identified on the seismic profile (trend for the fault F1 is inferred). *Thick black line* = location of the seismic profile described in this paper; fine *red lines* = ship track during the ATACAMES cruise. **b** Seismic profile front of the Cape Galera (location Fig. 8a). Red lines are limits between units; green lines are faults. *Thick black dashed line* = sea-bottom first multiple. *Black arrow* = shelf break

probably contributes to the good preservation of the canyon filling stages meanwhile its wide shelf probably reduces sediment transport during highstand times. The relatively flat seafloor morphology of the last canyon fill, which drape the canyon floor and the slope, (i.e. the absence of recent incision) suggests that little sediment transits in the canyon during the present day sea level highstand, thus corroborating this hypothesis. A decrease in the slope gradient of the canyon, due to tectonic deformation, might also lead to an aggrading sedimentation pattern in the canyon but the

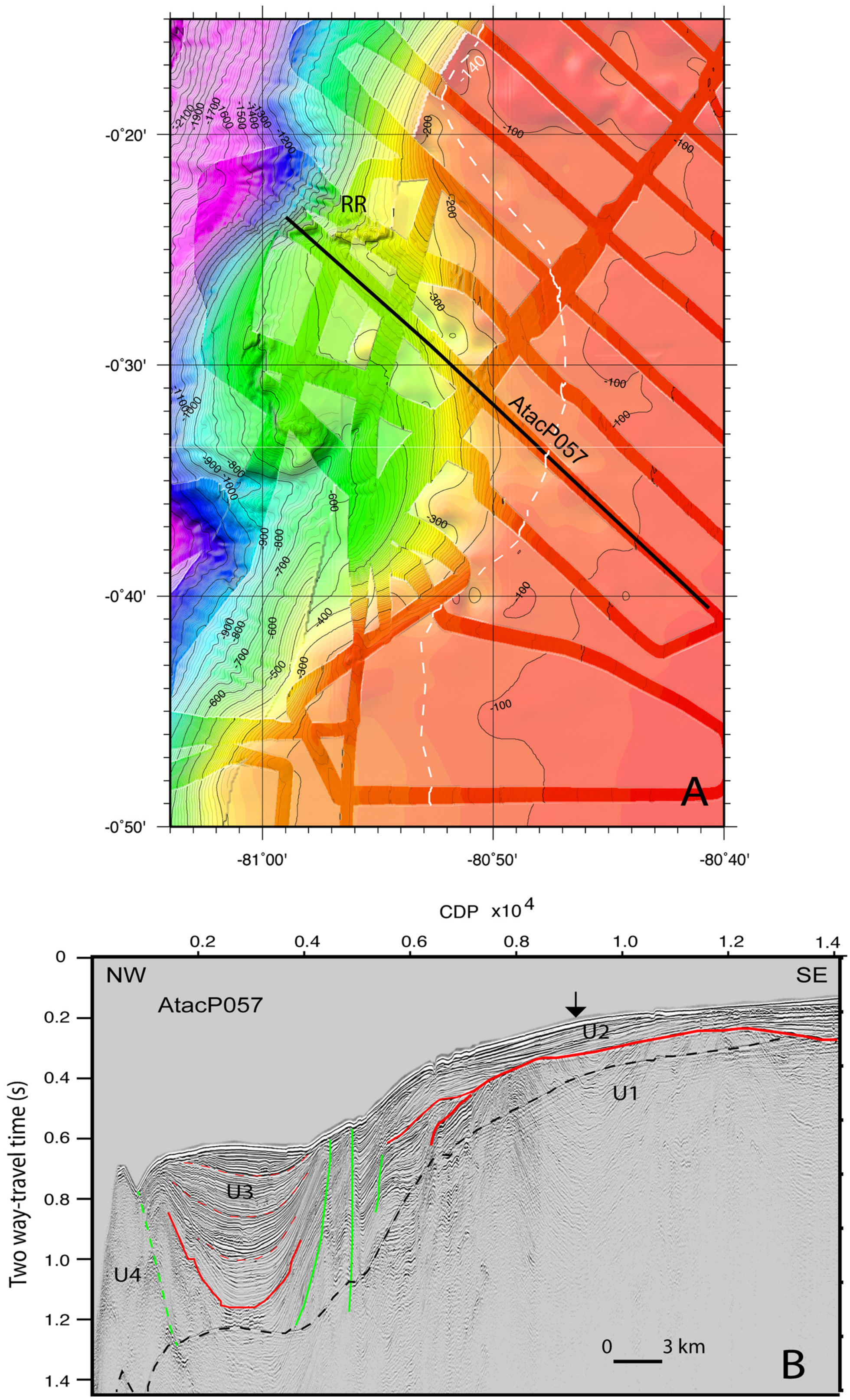

Fig. 9 **a** Bathymetric map of the continental platform of the Jama area (location on Fig. 3). More intense color corresponds to multibeam data recorded during the campaign ATACAMES with curves every 10 m. Less intense color with curves every 20 m = older multibeam data from Michaud et al. 2006; less intense *color* with curves every 100 m = area without multibeam. The white contour line corresponds to the isobaths -140 m contoured from ATACAMES data, which underlined a reentrant toward the east. RR = rough morphology (see text). *Thick black line* = location of the seismic profile describe in this paper; fine *red lines* = ship track during the ATACAMES cruise**.** **b** Seismic profile in front of Jama area (location Fig. 9a). *Red lines* are limits between units; green lines are faults. *Thick black dashed line* = sea-bottom first multiple. *Black arrow* = break in the shelf corresponding to isobaths -140 m

rates of creation of accommodation space due to tectonic deformation is much less than the rate of creation of accommodation space due to eustatic changes during Pleistocene times including on active subduction margins (Proust and Chanier 2004). The Santa Elena canyon is not related to a large onshore watershed on the contrary to

Esmeraldas and Guayaquil canyons. This canyon is smaller than the Esmeraldas and Guayaquil canyons and its sea-floor incision is less pronounced (Fig. 3). On the upper slope the course of the canyon is oriented NNE-SSW, sub-parallel to the shelf break, and probably controlled by fault F1 identified on AtacP110 profile. The NNE-SSW trend of this fault is the same than the Jipijapa fault trend (Fig. 3) known onland further north (Eguez et al. 2003; Bethoux et al. 2011; Reyes, Michaud 2012). In the recent past, it might have drained the coastal cordillera and the origin of the canyon is still conjectural. It should have evolved either by downslope incision by gravity flow or by upslope ret-rogressive erosion. The latter is however more likely as the Santa Elena canyon on the upper slope is guided by a fault might have drained currents and sediment pathways.

Vertical motions

The new multibeam bathymetry shows that the average water depth of shelf break (steepening of the gradient between the continental shelf and the upper continental slope) is at 160 m in the Gulf of Guayaquil, while north-ward of the gulf, along the Ecuadorian margin, it is located at c. 140 m and by places, like in Esmeraldas area at 110 m. This fits well with the fact that the Gulf of Guayaquil is known to be subsident during Pleistocene time (Deniaud et al. 1999; Witt et al. 2006; Witt and Bourgois 2009). The 140 m-deep shelf break corresponds to the last lowstand of sea level (Camoin et al. 2004), this suggesting a subsidence rate of about 0.11 cm/year for the shelf break of the northen margin since the 18,000 years ago (Bard et al. 1996) and 0.22 cm/year for the shelf break of the Gulf of Guayaquil by considering a current depth of 160 mbs.

In front of the Manta peninsula, the seismic data col-lected along the bathymetric reentrant (Fig. 7a) supports an overall subsidence of the shelf onlapped by a set of very well-preserved seismic sequences. These sequences, which display a similar internal architecture when compared to each others, are truncated by the last marine transgressive wave ravinement surface (3–6 k years). They are very likely of Pleistocene age and possibly as old as at least 800 k years for the lower one. This geometry and sediment history fit well with the reentrant shape of the upper margin slope. Landward of this subsidence area, eight marine terraces cover the main part of the Manta peninsula (Pedoja et al. 2006a). The hinge line between the onshore (uplifted) and offshore (subsided) areas may be associated with a fault that has remained so far undiscovered in absence of apropriate seismic data. Alternatively this pattern might be accounted for by a seaward tilting of the whole area. In this case, the upper surface of clinoforms should show a pro-gressive time-related tilt, decreasing from the oldest to the youngest ones. Nevertheless the geometry the clinoform upper boundaries (Unit 5 and 6 for exemple) show no clear tilt towards the ocean (Fig. 7b). The deepest and likely oldest clinoform U1 observed on seismic line P092 is located farther down slope at a water depth of 1 s. TWTT, i.e. ~750 m (Fig. 7b). Considering that this clinoform deposited near sea-level during an early-to mid-Pleistocene glacio-eustatic cycle, the shelf experienced a 750 ± 50 m subsidence. In such a scenario, the stack of 10 clinoform bodies each of them being tentatively associated with a ~100 Ka glacio-eustatic cycle (Camoin et al. 2004), might have recorded a ~1 Ma subsidence with an average rate of ~0.75 mm/year. By comparison, the onshore uplift rate in Manta peninsula is 0.42 mm/year (Pedoja et al. 2006a). These vertical deformation rates, although crude, are of the same order of magnitude and hence, call for a common driver.

Around La Plata Island both bathymetry and seismic reflection data indicate that this area has been uplifted concurrently with La Plata Island, where marine terraces are present (Cantalamessa and Di Celma 2004; Pedoja et al. 2006b). These marine terraces were cut in the basalts and dolerites of the Pinon Formation, which possibly cor-respond to the chaotic seismic facies of the rocks out-cropping at the shelf sea floor (Fig. 7c). The lack of accommodation space, forced the sediments to prograde beyond the shelf edge on the upper slope (Fig. 7c). This sedimentary geometry may be explained by a general uplift of the platform rather than a drop in absolute sea level as the margin uplift is clear at the nearby of La Plata Island (Pedoja et al. 2006b).

In the La Plata Island–Manta peninsula area, the new ATACAMES data show the juxtaposition of uplifted and subsided zones. The vertical movements can be due to local factors, possibly related to the topography of the subducting Carnegie Ridge: at the latitude of the Manta peninsula a subducting down-going plate topographic asperity might be responsible for the uplif of the Manta peninsula and associated subsidence of the adjacent seg-ment of the shelf.

In the Esmeraldas canyon area, the sedimentary archi-tecture showing seaward dipping, parallel-bedded, and faulted U3 and U4 units, suggests an overall seaward tilt of the sedimentary units and relative landward uplift. The U3 to U5 units are deeply incised by a set of paleochannels and a paleocanyon. The uplift is corroborated by (1) the well-stratified reflections in U5 prograding in a seaward direc-tion caused by a net baselevel fall, capped by channel incisions on the shelf and onlapped by the basal reflections of U6 on the slope and by (2) the present day highest location of the shelf edge in front of the Esmeraldas river outlet (110 m) compared with the shelf edge location on the promontary to the west (140 m).

Faults across the shelf

On one deep MCS profile, Collot et al. (2004) interpreted a flower structure offshore the onland Jama fault. This fault is interpreted as a major crustal transtensional strike-slip fault, trending NE-ward (Fig. 3). It represents a key element of the sismo-tectonic segmentation of the margin (Daly 1989). In the same area, the ATACAMES data show, a deformed sedimentary basin controlled by highly dipping faults (Fig. 9a); seismic profile in fig. 9b indicates that the faults tend to coalesce downward supporting the ''flower structure'' hypothesis. Moreover, Line P057 suggests that some of the faults have had a recent activity with a local compressive component affecting the most recent sediments and the seafloor. This supports the suggestion of an active transcurent fault extending the Jama fault in the offshore.

Northward and onland in the Galera area, several SW-NE trending faults (Fig. 8a) are reported (Pedoja et al. 2006a; Reyes and Michaud 2012) including the Galera fault (Fig. 3) that might be a transcurrent dextral fault (Eguez et al. 2003). These onshore faults do not extend across the shelf or at least do not affect the most recent unit as shown by seismic line ATAC P034 (Fig. 8). Nevertheless, seismic line P034, which cuts across the shelf break and the upper slope, provides evidences for a graben controlled by faults F1 and F2 that both show opposite dips; Although the F1 fault hanging-wall shows a complex deformation pattern including some evidence for contraction, the fault F1 is dominantly extensional and controls location of the graben southern flank. Active F2 fault scarp trends SW–NE similarly (Fig. 8b) to the onshore Galera faults system suggesting that the active F1–F2 fault system, which might reflect the surface expression of a negative flower structure, could represent a northward prolongation of the Galera faults system.

The Ecuadorian forearc is characterized by strike-slip tectonic environment since Paleocene until upper Miocene (Deniaud 2000; Daly 1989). Recent tectonic behaviour of the active margin of Ecuador during the early Pleistocene is associated with the northward migration of the North Andean Block (Witt et al. 2006). Geometry of the newly discovered faults in Galera and Jama areas suggests that are possibly strike slip faults. We do not know how long these inferred strike-slip faults worked and their rate of movement. We assume that these faults are strike slip faults and we suggest that they correspond to old faults reactivated by the subduction or coeval with the northward migration of the North Andean Block.

Conclusion

The ATACAMES data provide new constrains on the recent evolution of the Ecuadorian shelf in response to both climate change and tectonic deformation of the margin. The sedimentary records Pleistocene variations of sea level (i.e. climate change) is a powerful tool to evidence, to date and to quantify the impact of the tectonic deformation. The Guayaquil canyon shows a succession of episodes of sediment deposition and incision. The incision pattern records a relative fall and rise in base level with sediment fill preserved during the marine transgression. The Esmeraldas canyon is characterized by a major tributary breaching a narrow shelf towards the present day river outlet and a high activity of bottom currents dragging the river sediment through the shelf to the deep trench. The Santa Elena canyon on the upper slope appears guided by a SSW–NNE trending fault.

Several areas of the margin record vertical motion. In the Esmeraldas canyon area we evidence an uplift of the shelf. In the Manta peninsula- area, the shelf shows a likely Pleistocene subsidence of $\sim$750 m close to the Manta peninsula which in turn has been uplifted 300 m over the Pleistocene. The origin and the nature of the tectonic control of the hinge line is still a matter of debate. The vertical movements can be due to local factors, possibly related to the topography of the subducting Carnegie Ridge. We evidence the presence of two active fault systems on the shelf and upper margin slope. These faults with a possible transcurrent component located at the offshore prolongation of the onshore Jama and Galera faults systems. This strike-slip tectonic environment may be associated with a reactivation of older strike slip faults.

As indicated by the example of the La Plata Island Manta Peninsula areas, the ATACAMES data set has strong potential to quantify the along strike variations of the vertical motion of the Ecuadorian margin shelf.

Acknowledgments We thank the crew of R/V *L'Atalante* and GENAVIR. This work was supported by Institut National des Sciences de l'Univers du Centre National de la Recherche Scientifique (INSU). Thanks to Institut de la Recherche et du Développement (IRD), the Laboratoire Mixte International "Séismes et Volcans" (LMI) and to the Instituto Oceanográfico de la Armada (INOCAR). This work was partially sponsored by the Prometeo Project of the Ministry of Higher Education, Science, Technology and Innovation of the Republic of Ecuador (SENESCYT). We thank the two anonymous reviewers for their improvements.

References

Bard E, Hamelin B, Arnold M, Montaggioni L, Cabioch G, Faure G, Rougerie F (1996) Deglacial Sea level record from Tahiti corals and the timing of deglacial meltwater discharge. Nature 382:241–244

Bethoux N, Segovia M, Alvarez V, Collot JY, Charvis P, Gailler A, Monfret T (2011) Seismological study of the central Ecuadorian margin: evidence of upper plate deformation. J S Am Earth Sci 31:139–152

Bourgois J (2013) A review on tectonic record of strain buildup and stress release across the andean forearc along the gulf of guayaquil-tumbes basin (GGTB) near ecuador-peru border. Intern Journ Geosc 4:618–635. doi:10.4236/ijg.2013.43057

Camoin GF, Montaggioni LF, Braithwhite CJR (2004) Late to post glacial sea levels in the Western Indian Ocean. Mar Geol 206:119–146

Cantalamessa G, Di Celma C (2004) Origin and chronology of Pleistocene marine terraces of Isla de la Plata and of flat, gently dipping surfaces of the southern coast of Cabo San Lorenzo (Manabí, Ecuador). J S Am Earth Sci 16:633–648

Collot JY, Charvis P, Gutscher MA, Operto S (2002) Exploring the Ecuador-Colombia active margin and inter-plate seismogenic zone. EOS Trans AGU 83(17):189–190

Collot JY, Marcaillou B, Sage F, Michaud F, Agudelo W, Charvis P, Graindorge D, Gutscher MA, Spence G (2004) Are rupture zone limits of great subduction earthquakes controlled by upper plate structures? Evidence form MCS data acquired accross the N-Ecuador-SW Colombia margin. J Geophys Res 109:B11103. doi:10.1029/2004JB003060

Collot JY, Migeon S, Spence G, Legonidec Y, Marcaillou B, Schneider JL, Michaud F, Alvarado A, Lebrun JF, Sosson M, Pazmino A (2005) Seafloor margin map helps in understanding subduction earthquakes. EOS Trans AGU 86(46):463–465

Collot JY, Legonidec Y, Michaud F, Marcaillou B, Alvarado A, Ratzov G, Sosson M, Lopez E, Silva P, y el personal científico y técnico del INOCAR (2006a) Mapas del margen continental del Norte de Ecuador y del Suroeste de Colombia: Batimetría, Relieve, Reflectividad Acústica e Interpretación Geológica, publicación IOA-CVM-03-Post, 2006

Collot JY, Michaud F, Legonidec Y, Calahorrano A, Sage F, Alvarado A, y el personal científico y técnico del INOCAR (2006b) Mapas del margen continental Centro y Sur de Ecuador : Batimetría, Relieve, Reflectividad Acústica e Interpretación Geológica, publicación IOA-CVM-04-Post, 2006

Collot JY, Agudelo W, Ribodetti A, Marcaillou B (2008) Origin of a crustal splay fault and its relation to the seismogenic zone and underplating at the erosional north Ecuador–south Colombia oceanic margin. J Geophys Res 113:B12102. doi:10.1029/2008JB005691

Collot JY, Michaud F, Alvarado A, Marcaillou B, Sosson M, Ratzov G, Migeon S, Calahorrano A, Pazmino A (2009) Visión general de la morfología submarina del margen convergente de Ecuador-Sur de Colombia: implicaciones sobre la transferencia de masa y la edad de la subducción de la Cordillera de Carnegie. In Collot JY, Sallares V, Pazmiño A (ed) Geologia y Geofisica Marina y Terestre del Ecuador. Publicacion CNDM-INOCAR-IRD, PSE001-09, Guayaquil, Ecuador pp. 47–74

Daly MC (1989) Correlations between Nazca/Farallon Plate Kinematics and forearc basin evolution in Ecuador. Tectonics 8(4):769–790

Deniaud Y (2000) Enregistrement Sédimentaire et Structural de l'Evolution Géodynamique des Andes Equatoriennes au Cours du Néogène : Etude des Bassins d'Avant-arc et Bilans de Masse, Dissertation, thèse Université Grenoble I, Grenoble (France), 243 p

Deniaud Y, Baby P, Basile C, Ordoñez M, Montenegro G, Mascle G (1999) Opening and tectonic and sedimentary evolution of the gulf of Guayaguil: neogene and Quaternary fore-arc basin of the south Ecuadorian Andes. Comptes Rendus à l'Académie des Sciences, Paris 328:181–187

Eguez A, Alvarado A, Yepes H, Machette M, Costa C, Dart R (2003) Database and map of Quaternary faults and folds of Ecuador and its offshore regions. US Geol Surv Open File Rep, 03–289

Graindorge D, Calahorrano A, Charvis P, Collot JY, Bethoux N (2004) Deep structures of the margin and the Carnegie Ridge, possible consequence on great earthquake recurrence interval. Geoph Res Lett 31. doi:10.1029/2003GL018803

Gutscher MA, Malavieille J, Lallemand S, Collot JY (1999) Tectonic segmentation of the North Andean margin: impact of the Carnegie ridge collision. EPSL 168:255–270

Jaillard E, Benitez S, Mascle G (1997) Les déformations paléogènes de la zone d'avant arc sud-équatorienne en relation avec l'évolution géodynamique. Bull Soc Géol France 168:403–412

Marcaillou B, Collot JY (2008) Chronostratigraphy and tectonic deformation of the North Ecuadorian-South Colombian offshore Manglares forearc basin. Mar Geol 255:30–44

Michaud F, Collot J-Y, Alvarado A (2006) López E y el personal científico y técnico del INOCAR, (2006) República del Ecuador, Batimetría y Relieve Continental, publicación IOA-CVM-02-Post. INOCAR, Guayaquil

Michaud F, Witt C, Royer JY, (2009) Influence of the Carnegie ridge subduction on Ecuadorian geology: reality and fiction: In Kay S, Ramos V, and Dickinson WR (eds) Backbone of the Americas: Shallow Subduction, Plateau Uplift and Ridge and terrane Collision. Geol Soc Am Memoir 204:217–228 doi:10.1130/2009.1204.10

Mitchum RM Jr, Vail PR, Sangree JB (1977) Seismic stratigraphy and global changes of sea level; Part 6 Stratigraphic interpretation of seismic reflection patterns in depositional sequences. AAPG Memoir 26:117–133

Nocquet JM, Mothes P, Alvarado A (2009) Geodesy, geodynamics and earthquake cycle in Ecuador. Geology and marine and onland Geophysics of Ecuador: from the continental coast to the Galapagos Islands. In Collot JY, Sallares V, Pazmiño A (eds) Geologia y Geofisica Marina y Terestre del Ecuador. Publicacion CNDM-INOCAR-IRD, PSE001-09, Guayaquil, Ecuador pp 83–94

Paquet F, Proust JN, Barnes PM, Pettinga JR (2009) Inner forearc sequence architecture in response to climatic and tectonic forcing since 150 ka: Hawke's Bay New Zealand. J Sedim Res 79(3–4):97–124

Paquet F, Proust JN, Pettinga JR, Barnes PM (2011) Controls on active forearc basin stratigraphy and sediment fluxes: the Pleistocene Hawke Bay. Bull. Soc. Geol. Amer, New Zealand. doi:10.1130/B30243.1

Pedoja K, Ortlieb L, Dumont JF, Lamothe M, Ghaleb B, Auclair M, Labrousse B (2006a) Quaternary coastal uplift along the Talara Arc (Ecuador, Northern Peru) from new marine terrace data. Mar Geol 228:73–91

Pedoja K, Dumont JF, Lamothe M, Ortlieb L, Collot JY, Ghaleb B, Auclair M, Alvarez V, Labrousse B (2006b) Plio-quaternary uplift of the manta peninsula and La Plata Island and the subduction of the Carnegie Ridge, central coast of Ecuador. J S Am Earth Sci 22:1–21

Posamentier HW, Erskine RD, Mitchum RM (1991) Models for submarine fan depo- sition within a sequence stratigraphic frameworks. In: Weimer, P, Link, M (eds.), Seismic facies and sedimentary processes of submarine fans and turbidite systems. Springer, Berlin, pp. 197–222

Proust JN, Chanier F (2004) The Pleistocene cape Kidnappers section in New Zealand: orbitally-forced controls on active margin sedimentation? J Quat Sci 19(6):591–603

Ratzov G, Sosson M, Collot JY, Migeon S (2012) Late quaternary geomorphologic evolution of submarine canyons as a marker of active deformation on convergent margins: the example of the South Colombian margin. Mar Geol 315–318:77–97

Reyes P, Michaud F (2012) Mapa Geologico de la Margen Costera Ecuatoriana (1500000) EPPetroEcuador-IRD (eds), Quito Ecuador

Sage F, Collot JY, Ranero CR (2006) Interplate patchiness and subduction-erosion mechanisms: evidence from depth migrated

seismic images at the Central Ecuador convergent margin. Geology 4:997–1000
Silva P A (2007) Analisis morphologico y estructural del cañon submarino del rio Esmeraldas a partir de datos de geofisica marina. Dissertation, Escuela Politecnica Nacional, Quito, Ecuador
Silva P, Collot JY, Michaud F, Alvarado A, Lebrun JF, Legonidec Y (2006) El cañón submarino Esmeraldas (Ecuador) : estructuras y evolución geológica a partir del análisis de datos de geofísica marina. In : Memorias : sextas jornadas en ciencias de la tierra. Quito : Escuela Politecnica Nacional, 2006:44–48
Trenkamp R, Kellogg JN, Freymueller JT, Mora P (2002) Wide plate margin deformation, southern Central America and northwestern South America, CASA GPS observations. J S Am Earth Sci 15:157–171
Vail, PR, Todd RG, Sangree JB, (1977) Seismic stratigraphy and global changes of sea level: part 5. chronostratigraphic significance of seismic reflections: section 2. Appl Seism Reflect Config Stratigrap Interpretat 26:99–116
Witt C, Bourgois J (2009) Forearc basin formation in the tectonic wake of a collision-driven, coastwise migrating crustal block: the example of the North Andean block and the extensional Gulf of Guayaquil-Tumbes basin (Ecuador-Peru border area). GSA Bull 122:89–108. doi:10.1130/B26386.1
Witt C, Bourgois J, Michaud F, Ordoñez M, Jiménez N, Sosson M (2006) Development of the Gulf of Guayaquil (Ecuador) as an effect of the North Andean Block tectonic escape since the lower Pleistocene. Tectonics 25. doi:10.1029/2004TC001723